An improved scale factor calibration model of MEMS gyroscopes

[1,2]Qijian Tang, [1]Xiangjun Wang, [2]Qingping Yang, [1]Changzheng Liu
[1]MOEMS Education Ministry Key Laboratory, Tianjin University, Tianjin 300072, P. R. China
[2]School of Engineering and Design, Brunel University, Uxbridge, Middlesex UB8 3PH, UK
ytqjtang@163.com,xdocuxjw@vip.163.com,Ping.Yang@brunel.ac.uk

***Abstract*—Scale factor nonlinearity is one of the main errors of MEMS gyroscopes. This paper firstly analyzes the operating principle of MEMS gyroscopes, and presents the commonly used model in calibration process. It is proved that calibrating the gyroscope scale factor in segments will result in higher fitting accuracy. Since it is difficult to determine the inverse function of a higher order function in microprocessor, this paper has developed a new calibration model, including the selection of suitable segment points based on the fitting residual error. The calibration experiments and validation test results have confirmed the high accuracy of this new model, with the calibration accuracy almost improved by one order of magnitude compared with the original model. It is also applicable to other MEMS gyroscopes.**

Keywords—MEMS gyroscope; scale factor; calibration process; segment point; fitting residual error

I. INTRODUCTION

MEMS gyroscopes as a kind of angular-rate sensor have been widely used due to its small size, light weight, low power consumption and low price. However, they tend to has low accuracy in practical applications since they are susceptible to a number of influence factors including scale factor errors, quantization effects, temperature effects, random drift and additive noise [1-3]. In particular, MEMS gyroscopes are sensitive to vibrations due to the required high quality factor (Q-factor). Whilst the high Q is beneficial in improving gyro performance, it may also increase output signal distortion and the effects from environment factors [4-5]. These errors manifest generally in three types: zero bias, scale factor nonlinearity and stochastic errors. Zero bias is susceptible to temperature, the structure error and circuit noises are the main causes of nonlinearity of scale factor. The stochastic errors include angle random walk, rate random walk, quantization, Markov noise, bias instability, etc. [6]. This paper focuses on the studies of scale factor and its calibration. In order to improve the accuracy, the common approach is to establish the error model and apply the compensation method[7-8]. This paper will firstly analyze the relationship between the gyroscope rate output and the rotary angular velocity, and then give a detailed description of the common compensation model. Based on the features of the microprocessor, this paper proposes an improved compensation model.

II. GYROSCOPE RATE OUTPUT ANALYSIS

Take a z-axis MEMS gyroscope for example. It has two perpendicular vibration directions, x axis and y axis, which are the drive mode and the test mode, respectively. The y axial vibration is caused by Coriolis force. When the gyroscope is powered on, the mass block, caused by periodic electrostatic force, will undergo harmonic vibration in x axis. If there is a certain angular velocity along the z axis, Ω, the mass will sense Coriolis force in y axis. And the angular velocity, Ω, can be calculated through the mass displacement in y direction.

It is considered that the mass vibration amplitude has a linear relationship with Ω. The common model for the gyroscope's rate output in terms of the rotary velocity and the zero bias is shown in (1) [9-10].

$$V = k * \omega + V_0 + k_0 + \xi \tag{1}$$

where

V is the gyroscope rate output;

V_0 is the zero bias;

ω is the rotary velocity input;

k is the scale factor;

k_0 is the nonlinear error;

and ξ is the random error.

In this paper, the zero bias has been compensated [11], without considering the temperature effect on scale factor temporarily [12]. Let $\Delta V = V - V_0$ and from (1), we have:

$$\Delta V = k * \omega + k_0 + \xi \tag{2}$$

Place the z-axis MEMS gyroscope on a high precision turntable, and conduct calibration under different rotary velocities $\omega_j (j = 1,2,3 \cdots n)$, We obtain:

$$\begin{bmatrix} \Delta V_1 \\ \Delta V_2 \\ \vdots \\ \Delta V_n \end{bmatrix} = \overline{k} * \begin{bmatrix} \omega_1 \\ \omega_2 \\ \vdots \\ \omega_n \end{bmatrix} + \begin{bmatrix} k_{01} \\ k_{02} \\ \vdots \\ k_{0n} \end{bmatrix} + \begin{bmatrix} \xi_1 \\ \xi_2 \\ \vdots \\ \xi_n \end{bmatrix} \tag{3}$$

where

$$\overline{k} = \begin{bmatrix} k_1 & 0 & 0 & 0 \\ 0 & k_2 & 0 & 0 \\ 0 & 0 & \ddots & 0 \\ 0 & 0 & 0 & k_n \end{bmatrix}.$$

Let the relationship between the gyroscope scale factor and the input rotary velocity, as shown in (4) [7].

$$k_g = k_{g0} + \sum_{i=1}^{m} k_{gi} * \omega^i \quad (i \le m) \tag{4}$$

The work was supported by Support Program of National Ministry of Education of China (No.625010110) and National Natural Science Foundation of China (No.61179043). It was also supported by China Scholarship Council.

where

m is the maximum order of the fitting equation.

It can be obtained from (2) and (4).

$$\Delta V = k_{g0} * \omega + \sum_{i=1}^{m} k_{gi} * \omega^{i+1} + k_0 + \xi \quad (i \leq m) \quad (5)$$

Thus the relationship between the rate output and the input velocity can be obtained by the least square fitting. Meanwhile, gyroscope's scale factor refers to the ratio of the rate output and the input velocity. The fitting residual reflects the credibility of the fitting data and represents the difference between the actual and calculated velocity [13].

The calibration data for a single axial gyroscope was obtained with a high precision turntable. The data was acquired when the environment temperature was stable, with the rotary velocity changing from -60°/s to 60°/s at a step of 3°/s. The rate data after zero bias compensation is shown in Fig.1.

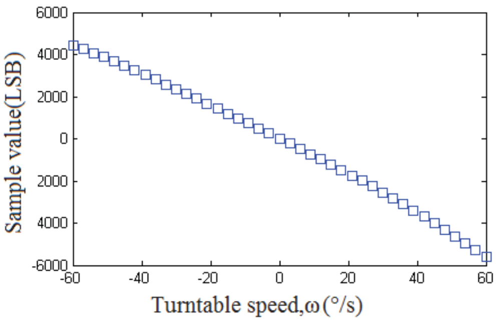

Fig. 1. Rate data points at different rotary velocities.

It is apparent that the fitting residual error is decreasing with the order of the model. However in practical applications, the processor gets the rotary velocity through the AD values. Thus (5) needs to be solved for the inverse function in high order fitting models. Considering handling capacity of the microprocessor, it is difficult to obtain the inverse function of the second or higher order equation. The commonly used solution to this problem is to use segmented one-dimensional equations [7,10,14]. As shown in (6).

$$\begin{cases} \Delta V_1 = k_{01} + k_{g01} * \omega \quad (\omega_1 < \omega < \omega_2) \\ \Delta V_2 = k_{02} + k_{g02} * \omega \quad (\omega_2 < \omega < \omega_3) \\ \vdots \\ \Delta V_n = k_{0n} + k_{g0n} * \omega \quad (\omega_n < \omega < \omega_{n+1}) \end{cases} \quad (6)$$

The experimental data points are divided into four segments. The three segment points are selected according to angular rate (Take 0°/s and ±10°/s as the segmented points for example). However the fitting residual error is still about 0.6°/s at some points, which is not acceptable. An improved model will be presented here to enhance the gyro calibration accuracy.

III. IMPROVED CALIBRATION MODEL

Rearrange (2) into another format.

$$\frac{1}{k} * \Delta V = \omega + \frac{1}{k} * k_0 + \frac{1}{k} * \xi \quad (7)$$

Make $k' = \frac{1}{k}$, while in velocity calibration process, it can be obtained:

$$\overline{k'} * \begin{bmatrix} \Delta V_1 \\ \Delta V_2 \\ \vdots \\ \Delta V_n \end{bmatrix} = \begin{bmatrix} \omega_1 \\ \omega_2 \\ \vdots \\ \omega_n \end{bmatrix} + \overline{k'} * \begin{bmatrix} k_{01} + \xi_1 \\ k_{02} + \xi_2 \\ \vdots \\ k_{0n} + \xi_n \end{bmatrix} \quad (8)$$

where

$$\overline{k'} = \begin{bmatrix} 1/k_1 & 0 & 0 & 0 \\ 0 & 1/k_2 & 0 & 0 \\ 0 & 0 & \ddots & 0 \\ 0 & 0 & 0 & 1/k_n \end{bmatrix}.$$

Then the relationship between the scale factors and the rate data acquisition values is established as (9).

$$k_g{}' = k_{g0}{}' + \sum_{i=1}^{m} k_{gi}{}' * \Delta V^i \quad (i \leq m) \quad (9)$$

From (9) and (7), it can be obtained:

$$\omega = k_{g0}{}' * \Delta V + \sum_{i=1}^{m} k_{gi}{}' * \Delta V^{i+1} + k_0{}' \quad (i \leq m) \quad (10)$$

where

$$k_0{}' = -\frac{k_0 + \xi}{k_g{}'}.$$

According to (10), the practical velocity is directly calculated, which does not need the inverse function and has simplified the calibration process. The segmented functions are shown in (11).

$$\begin{cases} \omega_1 = k_{01}{}' + \sum_{i=1}^{m} k_{g1i}{}' * \Delta V^i (\omega_1 < \omega < \omega_2) \\ \omega_2 = k_{02}{}' + \sum_{i=1}^{m} k_{g2i}{}' * \Delta V^i \quad (\omega_2 < \omega < \omega_3) \\ \vdots \\ \omega_n = k_{0n}{}' + \sum_{i=1}^{m} k_{gni}{}' * \Delta V^i \quad (\omega_n < \omega < \omega_{n+1}) \end{cases} \quad (11)$$

Meanwhile, selecting suitable segment points is another important problem. In general, the fitting accuracy increases with the number of segments. However, it is not realistic in practical applications. The references [7] and[14] select the segment points according the velocity, the reference [10] chooses the zero point as an segment point although it proposed to select the point through higher-order fitting function. This paper proposes to choose these suitable segment points through the extreme value point of fitting residual error.

IV. VALIDATION TEST

These data points are fitted by quadratic equation, and the velocity fitting residual line has three suitable extreme values at -42°/s, -9°/s and 33°/s. Thus these calibration data is divided into four segments, the comparison results are shown in Fig.2. Fig.2(a) shows the residual error decreases to less than 0.1°/s from above 0.3°/s before and after segmented fitting. Fig.2(b) indicates the comparison of the common model using (6) and the improved calibration proposed in this paper. The calibration accuracy has nearly been improved by one order of magnitude.

Another two sets of data were obtained at the rotary velocities of 25°/s and -25°/s, with 50000 points for each set. Before processing, these points are filtered by sliding mean filter. To verify the model developed in this paper, the data was used to calculate the rotary angular velocity according to (6) and (11). The results are shown in Fig.3. The experiments have demonstrated that the improved method presented is very effective.

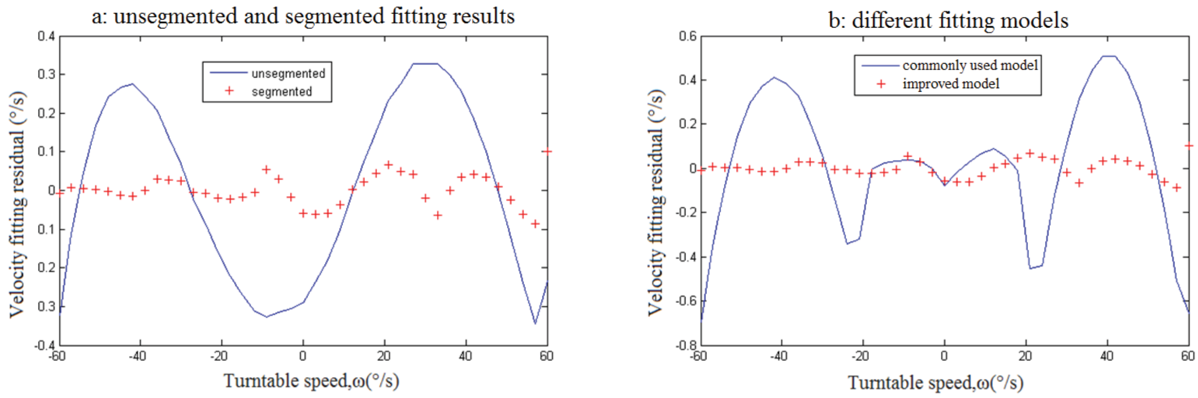

Fig. 2. Comparison results.

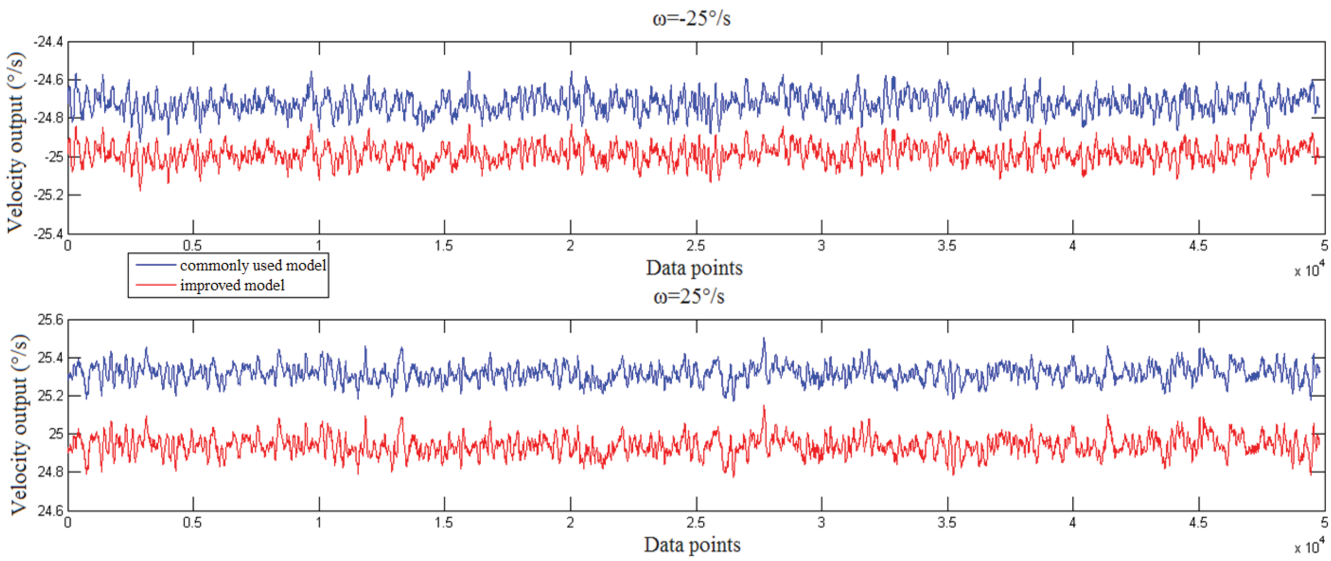

Fig. 3. Validation test results at the speeds of 25°/s and -25°/s.

V. CONCLUSIONS

Based upon the analysis of the common model of MEMS gyroscope's rate output and the turntable rotary velocity, the paper has shown that calibration of gyroscope's scale factor in segments will achieve higher fitting accuracy. As it is difficult to obtain the inverse function of higher order functions, this paper developed a new calibration method based on the original model. Further, this paper has proposed to choose the segment points based on the extreme values of the fitting residual error. Calibration experiments and validation test results demonstrated that the method established in this paper can achieve higher accuracy. The calibration accuracy is almost improved by one order of magnitude. The method can be used for the accurate calibration of the gyroscope in practical applications and is applicable to other MEMS gyroscopes.

REFERENCES

[1] H. Jiang, Q. Wei, H. Jia and X. Zhang, "Analysis of impact of gyroscope synthetical error on an electric-optical stabilized control system," International Conference on Biomedical Engineering and Informatics, pp. 2623-2625, 2010.

[2] V. Skvortzov, Y. Cho and B. Lee and C. Song, “Development of a gyro test system at Samsung Advanced Institute of Technology,” Position Location and Navigation Symposium, pp. 133 -142, 2004.

[3] R. Vaccaro and A. Zaki, “Statistical modelling of rate gyros,” IEEE Trans. Instr. Meas. vol.61, pp. 673-684, Mar. 2012.

[4] S. Yoon, S. Lee, K. Najafi, “Vibration-induced errors in MEMS tuning fork gyroscopes,” Sensors and Actuators A:Physical, vol. 180, pp. 32-44, Apr. 2012.

[5] D. Kim and R. M’Closkey, “Spectral analysis of vibratory gyro noise,” IEEE Sensors Journal, vol. 13, pp. 4361-4374, Nov. 2013.

[6] IEEE Aerospace and Electronic Systems Society, “IEEE standard specification format guide and test procedure for Coriolis vibratory gyros,” Technical Report, IEEE 952-1997, 2004.

[7] J. Li, J. Fang and W. Sheng, “Error analysis and integrated compensation of scale factor for MEMS gyroscope,” Journal of Beijing University of Aeronautics and Astronautics, vol. 33, pp. 1064-1081, Sept. 2007.

[8] S. Wang and G. Wu, “A summary of the methods for compensating temperature error of inertial devices,” Journal of Chinese Inertial Technology, vol. 6, pp. 44-49, 1998.

[9] B. Li, Y. Wu and C. Wang, “The identification and compensation of temperature model for hemispherical resonator gyro signal,” ISSCAA, Harbin, pp. 398-401, 2010.

[10] Z. Zhang, J. Xia and C. Cai, “Engineering realization of calibrating FOG’s scale factor in segments,” Journal of Chinese Inertial Technology, vol. 16, pp. 99-103, Feb. 2008.

[11] D. Keymeulen, C.Peay, K. Yee and D. Li, “Effect of temperature on MEMS vibratory rate gyroscope,” IEEE Aerospace Conference, pp. 1-5, 2005.

[12] J. Fang , J. Li and W. Sheng, “Improved temperature error model of silicon MEMS gyroscope with inside frame driving,” Journal of Beijing University of Aeronautics and Astronautics, vol. 32, pp. 1277-1303, Nov. 2006.

[13] C. Deng, “Calibration of MEMS gyro in strapdown inertial navigation system,” Ship Electronic Engineering, vol. 28, pp. 67-69, 2008.

[14] B. Liu and X. Li, “The research of real time and segmented error compensation of gyroscope in SIMU,” Aerospace Control, vol. 23, pp. 72-75, 2005.